Mesa S., Lina M.; Lasso, Carlos A.; Ochoa, Luz E.; DoNascimiento, Carlos
Trichomycterus rosablanca (Siluriformes, Trichomycteridae)
a new species of hipogean catfish from the Colombian Andes
Biota colombiana, vol. 19, no. 1, Suppl., 2018, pp. 95-116
Instituto Alexander von Humboldt

DOI: https://doi.org/10.21068/c2018.v19s1a09

Trichomycterus rosablanca (Siluriformes, Trichomycteridae) a new species of hipogean catfish from the Colombian Andes

Trichomycterus rosablanca (Siluriformes, Trichomycteridae) una especie nueva de bagre hipogeo de los Andes colombianos

Lina M. Mesa S., Carlos A. Lasso, Luz E. Ochoa y Carlos DoNascimiento

Abstract

Trichomycterus rosablanca is described as a new troglobitic catfish species from caves in southeastern Santander, Colombia. These caves are drained by the Carare River of the Magdalena River basin. The new species is characterized by the advanced condition in the typical troglomorphisms found in other congeneric cave-dwelling species, such as absence of eyes and pigmentation. *Trichomycterus rosablanca* is diagnosed by the following putative autapomorphies: 1) presence of a circular foramen in the main body of the interopercle, dorsal to the interopercular plate supporting the odontodes, and 2) presence of a single sensory pore in the posteriormost section of the infraorbital canal. *Trichomycterus rosablanca* can be distinguished from all known *Trichomycterus* species from Colombia by having the supraorbital canal interrupted in the nasal section, resulting in the pattern of s1, s2, s3, and s6 sensory pores, and the lachrimal/antorbital bone not enclosing the anteriormost section of the infraorbital canal. The genetic distinctiveness of *Trichomycterus rosablanca* is confirmed by GMYC and genetic distance method analyses of the cytochrome C oxidase subunit I gene sequence. The description of this species places Colombia as the second most diverse country in the continent in terms of number of cave fish species and calls the attention on the conservation efforts needed to guarantee the permanence of this remarkable diversity of hypogean fishes.

Keywords. Cave fish. Karstic. Middle Magdalena River basin. Santander.

Resumen

Se describe *Trichomycterus rosablanca*, una especie nueva de bagre troglobio de cuevas en el suroriente de Santander, Colombia. Estas cuevas son drenadas por el río Carare, de la cuenca del río Magdalena. La especie nueva se caracteriza por la condición avanzada en los troglomorfismos típicos encontrados en otros congéneres habitantes de cuevas, como ausencia de ojos y pigmentación. *Trichomycterus rosablanca* es diagnosticado por las siguientes autapomorfías putativas: 1) presencia de un foramen circular en el cuerpo principal del interopérculo, dorsal a la placa interopercular soportando los odontodes, y 2) presencia de un único poro sensorial en la sección más posterior del canal infraorbital. *Trichomycterus rosablanca* puede ser distinguida de todas las especies conocidas de *Trichomycterus* de Colombia por tener el canal supraorbital interrumpido en la sección nasal, resultando en el patrón de poros sensoriales s1, s2, s3 y s6 y el hueso lacrimal/antorbital no encerrando la sección más anterior del canal infraorbital.

La identidad genética de *Trichomycterus rosablanca* es confirmada por análisis GMYC y de distancia genética de la secuencia génica de la subunidad I de la citocromo C oxidasa. La descripción de esta especie ubica a Colombia como el segundo país más diverso en el continente en términos del número de especies de peces cavernícolas y llama la atención sobre los esfuerzos de conservación necesarios para garantizar la permanencia de esta extraordinaria diversidad de peces hipogeos.

Palabras clave. Cárstico. Cuenca media del río Magdalena. Pez cavernícola. Santander.

Introduction

Trichomycteridae is a family of Neotropical catfishes that includes 298 valid species, one fourth of which have been described in the last decade (Eschmeyer & Fong, 2017). The family is one of the most broadly distributed Neotropical fish groups, being found from Costa Rica to Patagonia, and on both sides of the Andes, from lowland streams of the Atlantic coast of Brazil to high elevation Andean streams and lakes at 4500 m a.s.l. (Arratia, 1983; de Pinna & Wosiacki, 2003). The most species-rich genus in the family is *Trichomycterus* Valenciennes, 1832, which is also widely distributed in the Neotropics, and comprises 176 valid species, 37 of which are distributed in Colombia (Eschmeyer & Fong, 2017). In general terms, the species of the genus in northern South America are distributed along the Andes, in the Pacific, Caribbean, and Orinoco flanks, in the Cordillera de la Costa of Venezuela, and in the Guiana Shield. Nonetheless, the highest diversity is found in the trans-Andean basin of the Magdalena-Cauca rivers in Colombia (DoNascimiento *et al*., 2014b).

Some *Trichomycterus* species have successfully invaded subterranean habitats, with nine described species that show a variable degree of development of the typical troglomorphic features: from eyes normally developed and densely pigmented skin, to absent eyes and unpigmented skin. From these nine cave inhabitants, *Trichomycterus chaberti* Durand, 1968 is the species found at the highest elevation (2800 m a.s.l.) in the southern Bolivian Andes; followed by *T. sketi* Castellanos-Morales, 2010 at 2157 m a.s.l. in a tributary of the Opón River, which empties into the middle basin of the Magdalena River in Colombia; *T. sandovali* Ardila-Rodríguez, 2006, *T. santanderensis* Castellanos-Morales, 2007, and *T. uisae* Castellanos-Morales, 2008, whose type localities are relatively close to each other, between 1000 to 1700 m a.s.l. in different tributary rivers of the Sogamoso River, of the middle basin of the Magdalena River; *T. dali* Rizzato, Costa, Trajano, and Bichuette, 2011 at 792 m a.s.l. in southeastern Brazil; *T. spelaeus* DoNascimiento, Villarreal, and Provenzano, 2001 distributed in the eastern flank of the Serranía de Perijá, in a tributary of the Lago de Maracaibo basin at 590 m a.s.l.; and *T. itacarambiensis* Trajano and de Pinna, 1996 and *T. rubbioli* Bichuette and Rizzato, 2012, both found at around 500 m a.s.l. in the Brazilian Atlantic basin of the São Francisco River. Here we describe a new species found between 2228 m and 2378 m of elevation from the headwaters of the Carare River, a tributary of the middle basin of the Magdalena River in Colombia.

Materials and methods

Examined specimens are deposited in the freshwater fish collection of the *Instituto de Investigación de Recursos Biológicos Alexander von Humboldt* (IAvH-P). Comparative material is listed in DoNascimiento *et al*. (2014a, b), DoNascimiento (2015), and García-Melo *et al*. (2016). Measurements and counts follow de Pinna (1992), with the addition of interopercular patch length (taken from base of anteriormost odontode to distal tip of posteriormost odontode). Measurements were taken on the left side of specimens with a digital caliper and rounded to the nearest decimal of

millimeter. Photographs of anatomical structures were taken with a digital camera Leica MC 190 HD attached to a stereomicroscope Leica S8APO, using the Leica Application Suite v. 3.3.0. Final edited figures are composite multifocal images of individual photographs stacked using the software Helicon Focus v. 6.7.1 Pro. Paratypes IAvH-P 14050 (59.5 mm SL), IAvH-P 15809 (48.8 mm SL), and IAvH-P 15813 (67.9 mm SL) were double-stained for bone and cartilage following Datovo and Bockmann (2010), and dissected on the right side of the head in order to expose the dorsolateral muscles of the head for descriptive and comparative purposes. These three specimens were then cleared (CS) following Taylor and Van Dyke (1985) for osteological study. Nomenclature of sensory pores of supraorbital, infraorbital, and otic canals followed Arratia and Huaquin (1995), and terminology and homologies for postotic branches follow Schaefer and Aquino (2000). Counts of opercular and interopercular odontodes, pharyngeal teeth, branchiostegal rays, vertebrae, ribs, fin rays, number and position of supporting elements of dorsal and anal fins, and data from other osteological features were obtained from CS paratypes. Number of specimens is given in parentheses for each count in variable meristics and counts corresponding to the holotype are indicated by an asterisk. Vertebral counts include only post Weberian vertebrae, and the compound caudal centrum (PU1+U1) was counted as a single element (Lundberg & Baskin, 1969). Morphological data for *Trichomycterus chaberti*, *T. dali*, *T. itacarambiensis*, *T. rubbioli*, and *T. santanderensis* were obtained from their respective original descriptions, complemented by photographs of lateral, dorsal, and ventral views and a lateral radiograph of the holotype of *T. chaberti*, available at the All Catfish Species Inventory (ACSI) Image Base website (Morris *et al*., 2006).

A set of 14 cytochrome C oxidase subunit I (COI) sequences of trichomycterids was obtained from Ochoa *et al.* (2017), including two newly added species (*Trichomycterus laucaensis* Arratia, 1983 and *Trichomycterus guacamayoensis* Ardila Rodríguez, 2018), all available at Genbank (Table 1). Species sequences compared in our genetic analyses were selected (according to their availability) following two main criteria: (1) trichomycterines that share with *Trichomycterus rosablanca*, an interrupted supraorbital canal at the nasal section (*Eremophilus mutisii* Humboldt, 1805, *T. laucaensis*, and *T. punctulatus* Valenciennes, 1846), and (2) troglobitic species of *Trichomycterus* from cave systems geographically close to the type locality of the new species (*T. sandovali* and *T. guacamayoensis*). In addition, sequences from northern trans-Andean species of *Trichomycterus* analyzed by Ochoa *et al.* (2017) and clustered into the clades D1 and D2 were incorporated, as well as representatives of other trichomycterine genera (*Bullockia*, *Ituglanis*, and *Scleronema*). The tree was rooted with *Copionodon pecten* de Pinna, 1992, a representative of the clade Copionodontinae+Trichogeninae, hypothesized as the sister group of remaining trichomycterids (Datovo & Bockmann, 2010; Ochoa *et al*., 2017).

Sequences were aligned using MUSCLE with the default parameters. Nucleotide composition, substitution pattern, and genetic distances were examined. The neighbor-joining (NJ) tree was estimated using the Kimura two-parameter model (K2P) of the base substitution (Kimura, 1980), including a bootstrap analysis (1000 replications) in MEGA 7.0 (Kumar *et al*., 2016). An ultrametric gene tree was generated through Beast 1.8.0 (Drumond *et al*., 2012) with the Yule prior and the lognormal relaxed molecular clock model that assumes that rates of molecular evolution are uncorrelated but lognormally distributed among lineages (Drummond *et al*., 2006). We implemented the generalized mixed Yule-coalescent analysis (GMYC) using the calibrated tree for species delimitation analysis. The GMYC was conducted in R v. 3.0.0 (R Development Core Team 2013), using the package "splits" (Species Limits by Threshold Statistics; http://r-forge.r-project.org/projects/splits) and standard parameters (interval = c: 0.1) with a single threshold that specifies the transition time between to within species branching.

Table 1. Voucher information, GenBank and BOLD accession codes for the samples analyzed in the present study.

Species	Catalog number	GenBank /BOLD
Bullockia maldonadoi	LBP 3112	KY857926
Copionodon pecten	LBP 17357	KY857929
Eremophilus mutisii	ANSP 11306	KY857931
Ituglanis parahybae	LBP 10730	KY807219
Scleronema minutum	LBP 3310	KY857957
Trichomycterus areolatus	LBP 3118	KY857964
Trichomycterus banneaui	LBP 19847	KY857969
Trichomycterus cachiraensis	LBP 19832	KY857971
Trichomycterus laucaensis	LBP 91501	MF804496
Trichomycterus punctulatus	ANSP 180733	KY857983
Trichomycterus rosablanca	IAvH-P 15811	MH407228/ CBIHS009-17
Trichomycterus ruitoquensis	LBP 19838	KY857984
Trichomycterus sandovali	LBP 19833	KY857985
Trichomycterus guacamayoensis	IAvH-P 13984	MH407227/ CBIHS010-17
Trichomycterus aff. *spilosoma*	LBP 19339	KY857942
Trichomycterus cf. *striatus*	LBP 19846	KY858003
Trichomycterus cf. *transandianus*	LBP 19844	KY857999

Results

Trichomycterus rosablanca, new species
urn:lsid:zoobank.org:pub:4ACC4A1E-39DF-4D40-A51A-0E023E02D37F

Figure 1. Left lateral, dorsal, and ventral views of *Trichomycterus rosablanca*, holotype, IAvH-P-16086, 95.5 mm SL; Colombia, Santander, El Peñón, Las Sardinas Creek, tributary of Horta River, Carare River drainage, Magdalena River basin. Scale bar = 1 cm. Photograph by Felipe Villegas.

Table 2. Morphometric data for holotype and paratypes (64) of *Trichomycterus rosablanca*. Standard length expressed in mm. Measurements 2 to 11 expressed as % of SL and 12 to 18 as % of head length. M: mean; R: range; SD: standard deviation.

	Trichomycterus rosablanca			
	Holotype	**R**	**M**	**SD**
1. Standard length	95.5	28.7-102.5		
2. Total length	116.3	113.0-122.1	117.7	1.5
3. Body depth	14.9	8.9-16.6	13.8	1.4
4. Predorsal length	60.6	55.8-64.2	58.9	1.5
5. Preanal length	71.1	65.7-72.6	69.3	1.5

Cont. **Table 2**. Morphometric data for holotype and paratypes (64) of *Trichomycterus rosablanca*. Standard length expressed in mm. Measurements 2 to 11 expressed as % of SL and 12 to 18 as % of head length. M: mean; R: range; SD: standard deviation.

	Trichomycterus rosablanca			
	Holotype	**R**	**M**	**SD**
6. Prepelvic length	54.8	50.8-59.9	56.1	1.4
7. Dorsal-fin base	11.8	9.8-14.2	11.3	0.9
8. Anal-fin base	8.3	6.2-12.0	8.5	0.9
9. Caudal-peduncle length	20.7	19.7-30.2	22.8	1.7
10. Caudal-peduncle depth	14.2	9.1-17.5	12.5	1.3
11. Head length	17.3	15.5-20.1	18.3	1.0
12. Head width	101.8	84.1-111.3	99.1	6.5
13. Head depth	55.7	45.9-63.1	55.0	4.2
14. Mouth width	52.1	36.3-54.2	46.4	3.4
15. Maxillary-barbel length	94.7	50.1-124.8	86.9	16.6
16. Nasal-barbel length	80.4	44.3-106.8	81.9	11.9
17. Rictal-barbel length	70.7	37.8-80.7	64.5	10.8
18. Interopercular-patch length	31.9	23.2-43.1	35.5	3.8

Holotype. IAvH-P 16086, 95.5 mm SL; Colombia, Santander, El Peñón, Las Sardinas Cave, Las Sardinas Creek, tributary of Horta River, Carare River drainage, Magdalena River basin, 2308 m a.s.l., 06°05'36.0"N 73°49'42.7"W; 20 Aug 2016, Lina M. Mesa S. and Michael Galeano.

Paratypes. 70 specimens from Colombia, Santander, El Peñón, Carare River drainage, Magdalena River basin. IAvH-P 14050, 1 CS (59.5 mm SL); vereda El Venado, Sardina Creek, *ca*. 25 m outside the cave, 06°05'35.2"N 73°49'43.2"W, 2228 m a.s.l.; 26 Aug 2016, Carlos A. Lasso. IAvH-P 15806, 1 (50.8 mm SL); Caracol Cave, hypogean stream tributary of Horta River, 2378 m a.s.l., 06°05'14.3"N 73°49'54.3"W; 25 Aug 2016, Carlos A. Lasso, Camilo Martínez-Martínez, Camilo Chica, and Mario García. IAvH-P 15808, 1 (76.2 mm SL), collected with IAvH 15806. IAvH-P 15809, 19 (28.7-58.6 mm SL), 1 CS (48.8 mm SL), Las Sardinas Cave, hypogean stream tributary of Horta River, 2228 m a.s.l., 06°05'35.2"N 73°49'43.2"W; 25 Aug 2016, Carlos A. Lasso, Camilo Martínez-Martínez, Camilo Chica, and Mario García. IAvH-P 15810, 2 (50.1 mm SL), same locality as IAvH-P 15806; 19 Oct 2016, Lina M. Mesa S., Michael Galeano, and Rodrigo Barbella. IAvH-P 15811, 5 (48.7-74.8 mm SL), collected with the holotype. IAvH-P 15812, 17 (44.1-102.5 mm SL), same locality as

IAvH-P 15809; 19 Oct 2016, Lina M. Mesa S., Michael Galeano, and Rodrigo Barbella. IAvH-P 15813, 16 (41.2-77.7 mm SL), 1 CS (67.9 mm SL), collected at type locality; 19 Oct 2016, Lina M. Mesa S., Michael Galeano, and Rodrigo Barbella. IAvH-P 15814, 5 (45.6-65.5 mm SL), collected at type locality; 25 Aug 2016. Carlos A. Lasso, Camilo Martínez-Martínez, Camilo Chica, and Mario García. IAvH-P 15815, 1 (68.6 mm SL), collected with IAvH-P 15814.

Sequences. Genseq-2 COI: sequence of the mitochondrial gene cytochrome C oxidase subunit I of one paratype (IAvH-P 15811) of *Trichomycterus rosablanca* (genseq-2 COI following the nomenclature of Chakrabarty *et al*., 2013) is available through the following BOLD accession code: CBIHS009-17.

Diagnosis. *Trichomycterus rosablanca* is diagnosed by the following putative autapomorphies: 1) presence of a conspicuous circular foramen in the main body of the interopercle that communicates the lateral and medial surface of the bone (Figure 2) (*vs.* interopercle compact, lacking any foramina in other trichomycterines); 2) a single sensory pore in the posteriormost section of the infraorbital canal (*vs*. two sensory pores in the remaining *Trichomycterus* species). The new species can also be recognized from all Colombian species of *Trichomycterus*, including cave inhabiting congeners from northern South America (Colombia and Venezuela), by having the supraorbital canal interrupted at nasal region with a pattern of four sensory pores (s1, s2, s3, and s6) *vs*. supraorbital canal continuous with three sensory pores (s1, s3, and s6); and the lachrimal/antorbital bone compact, not enclosing the anteriormost section of the infraorbital canal (Figure 3) (*vs*. lachrimal/antorbital tubular and enclosing the anteriormost section of the infraorbital canal). *Trichomycterus rosablanca* is readily distinguished from epigean congeners and some hypogean species (*T. chaberti*, *T. itacarambiensis*, *T. rubbioli*, *T. sketi*, and *T. uisae*) by the absence of eyes and by having the body depigmented (except for *T. chaberti*, *T. rubbioli*, *T. sketi*, and *T. uisae*). The new species further differs from cave congeners from Colombia and Venezuela by having a relatively short nasal barbel, not surpassing the opercular patch of odontodes (*vs*. nasal barbel exceeding the base of the pectoral fin in *T. sandovali*, *T. santanderensis*, *T. sketi*, *T. spelaeus*, and *T. uisae*); 37 free vertebrae (*vs*. 35-36 in *T. sandovali* and *T. santanderensis*, 35 in *T. sketi* and *T. uisae*, and 34 in *T. spelaeus*). The new species differs from the hypogean species as follows: from *T. dali* by having a wider head (84.1-111.3% of HL *vs*. 44.2-74.9%); fewer branched pectoral-fin rays (7-8 *vs.* 9), pelvic-fin origin anterior to dorsal-fin origin (*vs.* at same vertical), absence of two conspicuous ridge-like adipose folds (one pre-dorsal and one post-dorsal), lining dorsally throughout the body (*vs.* folds present), anterior fontanel present (*vs.* absent), higher number of post Weberian vertebrae (37 *vs.* 34-35); from *T. itacarambiensis* by the absence of eyes (*vs.* eyes ranging from vestigial to fully developed), higher number of branched pectoral-fin rays (7-8 *vs.* 5-6), basypterigia bilaterally symmetrical and normally developed (*vs.* basypterigia asymmetrical and deformed); from *T. rubbioli* by having a higher number of post Weberian vertebrae (37 *vs.* 31-32) and hypural 3 separate from hypurals 4+5 (*vs*. partially fused); from *T. sandovali* by having the pelvic-fin origin anterior to the dorsal-fin origin (*vs.* at same vertical or slightly posterior), distal margin of pelvic fin not covering the urogenital papilla (*vs.* urogenital papilla completely covered by the pelvic fin), epiphyseal bar distinctively broader than the length of the anterior fontanel (*vs*. slender) (Figure 4), autopalatine with concave lateral margins and posterolateral process posteromedially curved with distal tip rounded (*vs*. lateral margins parallel and straight, posterolateral process triangular, posterolaterally oriented and distal tip pointed) (Figure 5), and lateral process of parurohyal slender and distally pointed (*vs*. wide and triangular in shape with distal tip rounded) (Figure 6); from *T. santanderensis* by having the pelvic-fin origin anterior to the dorsal-fin origin (*vs.* at same vertical), inner margins of pelvic-fin bases in contact (*vs*. widely separated, about 45% of pelvic-fin base length), posterior tip of fin

reaching urogenital papilla (*vs*. reaching anal-fin origin); from *T. sketi* by the distal margin of the pelvic fin not covering the urogenital papilla (*vs.* urogenital papilla completely covered by the pelvic fin), posterior fontanel complete (Figure 4) (*vs*. fontanel divided in two triangular openings connected through a midsagittal suture), autopalatine with concave lateral margins and posterolateral process posteromedially curved with distal tip rounded (*vs*. lateral margins parallel and straight, posterolateral process posterolaterally oriented and distally pointed), and lateral process of parurohyal slender and distally pointed (*vs*. wide and triangular in shape with distal tip rounded); from *T. spelaeus* by having a shallower body (8.9-16.6% of SL *vs*. 20.1-20.4%), a wider mouth (36.3-54.2% of HL *vs*. 31.6-33.9%), pelvic-fin origin anterior to dorsal-fin origin (*vs.* at same vertical), and distal margin of pelvic fin not covering the urogenital papilla (*vs.* urogenital papilla completely covered by the pelvic fin); from *T. uisae* by the distal margin of the pelvic fin not covering the urogenital papilla (*vs.* urogenital papilla completely covered by the pelvic fin) and anal-fin origin entirely behind dorsal-fin base (*vs*. at level of last dorsal-fin ray).

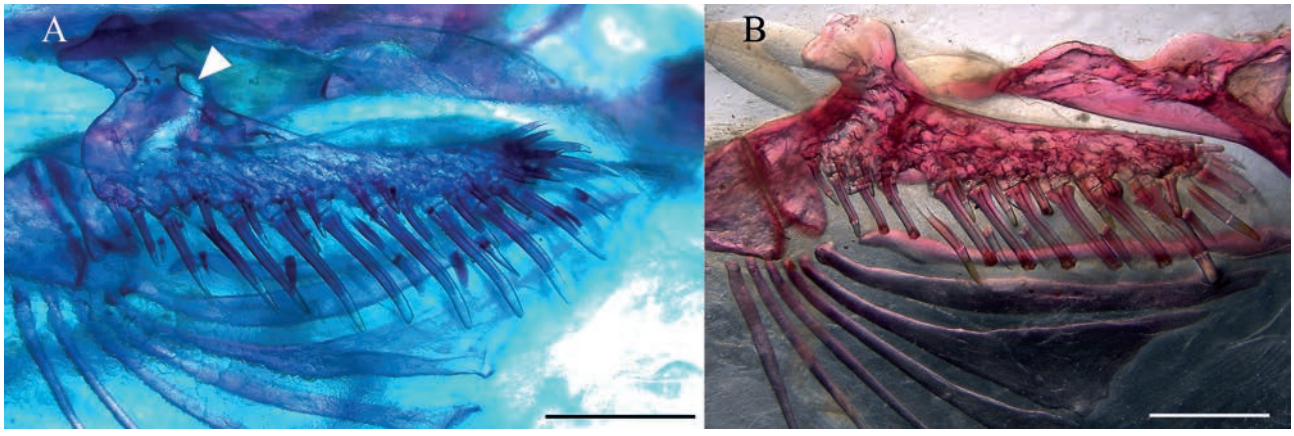

Figure 2. A. Left interopercle of *Trichomycterus rosablanca*, paratype, IAvH-P 15809, 48.8 mm SL, showing foramen (arrow head). B. Right interopercle of *T. sandovali* (horizontally flipped for ease of comparison), paratype, CAR 115, showing plesiomorphic character state, lacking foramina. Scale bar = 1 mm.

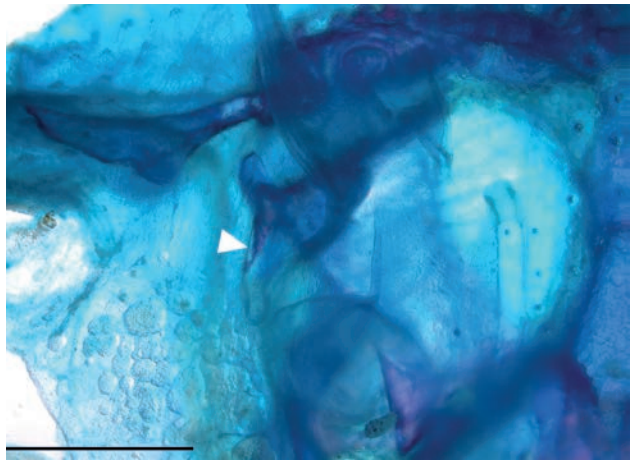

Figure 3. Left lachrimal/antorbital of *Trichomycterus rosablanca*, paratype, IAvH-P 15809, 48.8 mm SL, not enclosing infraorbital canal (arrow head). Scale bar = 1 mm.

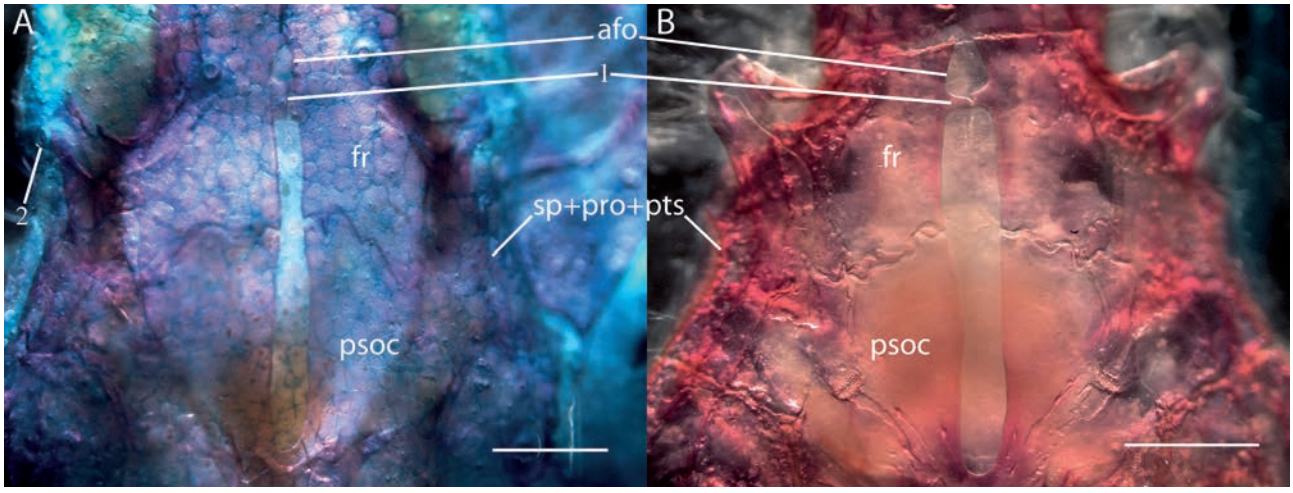

Figure 4. Dorsal view of posterior region of neurocranium of A. *Trichomycterus rosablanca*, paratype, IAvH-P 15809, 48.8 mm SL. B. *Trichomycterus sandovali*, paratype, CAR 115, showing 1. epiphyseal bar, 2. single sensory pore of posteriormost section of infraorbital canal. Scale bar = 1 mm. Abbreviations: afo, anterior fontanel; fr, frontal; psoc, parieto-supraoccipital; sp+pro+pts, sphenotic-prootic-pterosphenoid complex bone.

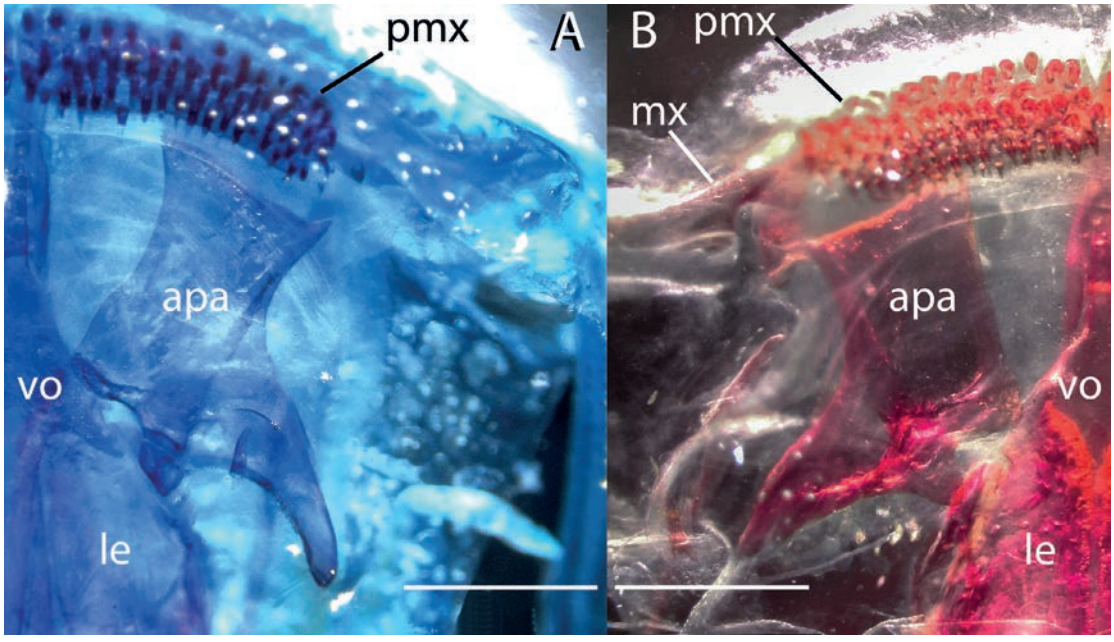

Figure 5. Ventral view of anterior region of neurocranium of A. *Trichomycterus rosablanca*, paratype, IAvH-P 15809, 48.8 mm SL. B. *Trichomycterus sandovali*, paratype, CAR 115. Scale bar = 1 mm. Abbreviations: apa, autopalatine; le, lateral ethmoid; mx, maxilla; pmx, premaxilla; vo, vomer.

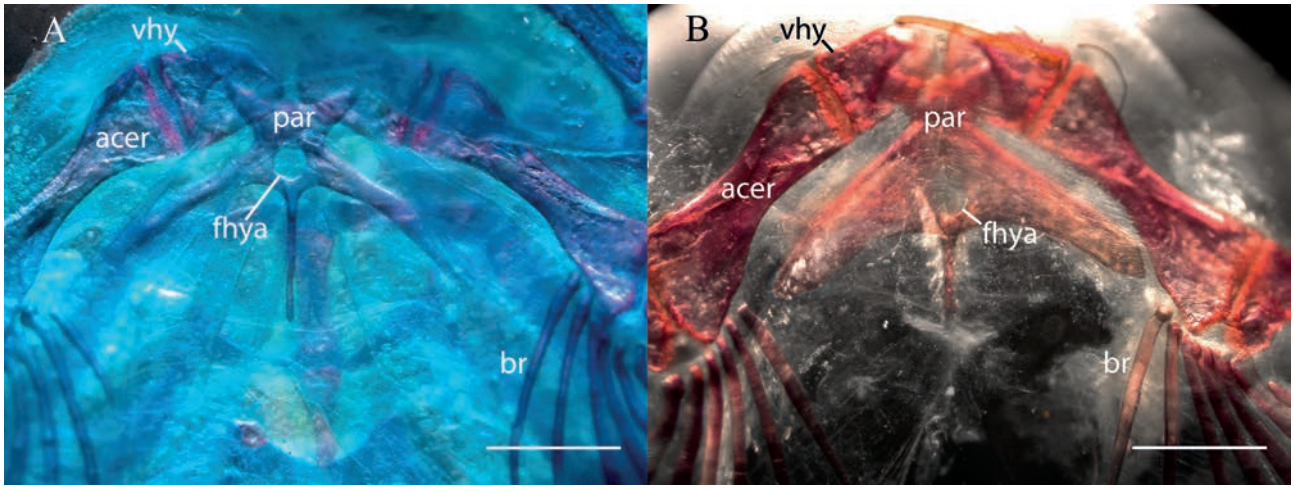

Figure 6. Dorsal view of hyoid arch of A. *Trichomycterus rosablanca*, paratype, IAvH-P 15809, 48.8 mm SL. B. *Trichomycterus sandovali*, paratype, CAR 115. Scale bar = 1 mm. Abbreviations: acer, anterior ceratohyal; br, branchiostegal rays; fhya; foramen for hypobranchial artery; vhy, ventral hypohyal; par, parurohyal.

Description. Morphometric data presented in Table 1. Body elongated, nearly as deep as wide, gradually compressed posterior to dorsal-fin base. Dorsal profile of head straight and inclined upward, then straight to slightly convex just posterior to head to dorsal-fin origin and slightly concave along dorsal-fin base; right after dorsal fin-base, continues straight or slightly convex along caudal peduncle. Ventral profile straight to end of pectoral-fin base, straight to slightly convex to anal-fin origin, then abruptly sloping dorsally along anal-fin base and straight and sloping ventrally along caudal peduncle. Cross-section of body circular at pectoral-fin insertion. Body encircled by tegumentary rings almost until midlength of caudal peduncle, after preservation of specimens in ethanol.

Head depressed, almost as wide as long, trapezoidal in dorsal view. Eyes absent. Mouth subterminal. Lateral fleshy lobe of lower lip rounded. Premaxilla with four irregular rows of conical teeth. Dentary with four irregular rows of teeth, similar to those of premaxilla. Anterior nostril surrounded by low fleshy thin flap, higher posteriorly and laterally continuous with nasal barbel. Posterior nostril anteriorly framed by fleshy elevated margin, decreasing in high posteriorly and leaving a posterior notch. Barbels dorsoventrally flattened and tapered distally. One specimen of 51.9 mm SL (IAvH-P 15812) with right maxillary barbel basally branched, both branches of similar length. Nasal barbel originating from lateral margin of anterior nostril, almost reaching base of opercular patch of odontodes. Maxillary barbel extending to pectoral-fin insertion. Rictal barbel extending to posterior margin of fleshy flap of interopercular patch of odontodes. Interopercular patch with 24-31 odontodes and 10-15 replacement odontodes, arranged in two irregular rows. Posterior interopercular odontodes of medial row largest and slightly curved medially at tip. Opercle with 11-14 odontodes and 3-5 replacement odontodes, disposed in approximately 5 anteroposterior irregular rows. Posteriormost opercular odontodes largest. Branchial membrane united across isthmus and supported by 7 branchiostegal rays (one CS specimen with six branchiostegal rays on right side). Branchiostegal rays 4-7 distally expanded. Branchiostegal ray 5 with greatest distal expansion.

Posterior portion of *levator internus 4* originating from dorsal surface of posttemporo-supracleithrum. Origin of *extensor tentaculi* from

neurocranium only. Insertion of secondary-ventral section of *dilatator operculi* restricted to posterior region of opercle. Primary section of *dilatator operculi* passing medial to *levator arcus palatini*.

Anterior margin of mesethmoid almost straight with a slight mesial concavity. Anterior fontanel small ovoid opening slightly shorter than epiphyseal bar. Lachrimal/antorbital not enclosing anterior section of infraorbital canal (sensory pores i1 and i3), but attached antero-ventrally (Figure 3). Sesamoid supraorbital as a long straight rod, without lateral processes, attached posteriorly to dorsoposterior corner of lateral ethmoid. Lateral process of frontal and sphenotic, where infraorbital canal leaves neurocranium, forming conspicuous anterolaterally projected postorbital process. Posterior fontanel rectangular in shape and long, *ca*. 9-10 times longer than anterior fontanel, extending anteriorly between posterior region of frontals and reaching posteriorly last third of parieto-supraoccipital (Figure 4A). Epiotic with smooth margins. Posttemporo-supracleithrum with long pointed anterior process, running along posteromedial margin of base of wing-like lateral process of pterotic and lying dorsal to center of pterotic. Medial process of posttemporo-supracleithrum attached directly to ventral surface of anterolateral region of Weberian capsule and ending in a pointed tip close to basi-exoccipital. Vomer arrow shaped with relatively short posterior process (not exceeding posteriorly anteromedial junction of orbitosphenoids) inserted into anterior process of parasphenoid. Lateral process of vomer slightly bifid, with posterior arm longer. Posterior process of parasphenoid long and extending over anterior portion of basi-exoccipital, laterally bordered by two extensive anterior membranous processes of basi-exoccipital. Optic foramen present but reduced to a small orifice in posterior region of orbitosphenoid, close to articulation with frontal. Lateral opening of Weberian capsule constricted at tip of lateral projection. Conspicuous convex lamina along posteroventral margin of lateral projection of Weberian capsule. Premaxilla almost rectangular in shape. Maxilla boomerang shaped and smaller than premaxilla. Dentary teeth extending posteriorly and stretching to a single row along basal half of coronoid process; 2-3 posteriormost teeth inserted posterior to vertical through articular facet of dentary for coronomeckelian cartilage. Ventral margin of dentary with small posteriorly curved process. Medial margin of autopalatine sinuous (Figure 5A). Posteromedial corner of autopalatine articulating with ventral facet at base of lateral process of vomer. Articular facet of autopalatine for lateral ethmoid on posterolateral corner of bone, just at base of posterolateral process. Variably developed laminar process extending medially from ventral surface of autopalatine at articulation with lateral ethmoid. Posterolateral process of autopalatine medially curved. Metapterygoid laminar and roughly rhomboidal in shape. Hyomandibula articulating anteriorly through dorsoanterior membranous outgrowth with metapterygoid. Anterior end of interopercular plate supporting odontodes, slightly posterior to articular facet of interopercle for preopercle. Posterior surface of main body of interopercle with a conspicuous rounded foramen at attachment point of interoperculo-opercular ligament (left interopercle of CS specimen IAvH-P 15813 lacking foramen). Opercular plate supporting odontodes relatively small, with a slender base connecting to main body of bone. Hypobranchial foramen large (Figure 6A). Lateral process of parurohyal long and uniformly slender for most of its length, ending in a pointed tip at level of midlength of posterior ceratohyal or reaching slightly beyond. Basibranchials 2 and 3 approximately of same length; hypobranchial 1 slightly shorter. Basibranchial 2 almost rectangular, with lateral margins slightly concave. Basibranchial 3 with anterior end twice wider than posterior end. Distal end of hipobranchial 1 slightly wider than proximal end. Anterolateral process of ossified portion of hypobranchial 3 blunt. Ceratobranchial 1 with 1-3 gill rakers at distal region of anterior margin. A single anterior gill raker at joint of ceratobranchial 1 and epibranchial 1. Anterior margin of epibranchial 1 with wide base triangular uncinate process, closer to distal end of epibranchial, and curved laterally. Posterior margin of epibranchial

1 with wide rectangular lamina and short process, close to distal end. Ceratobranchial 2 with 1-4 gill rakers along anterior margin. Epibranchial 2 with short wide base anterior uncinate process, 0-1 anterior gill raker close to joint with ceratobranchial 2, and short triangular posterior uncinate process close to distal end. Ceratobranchial 3 with 1-3 gill rakers along anterior margin, a broad notch at proximal portion of posterior margin and 5-8 gill rakers along posterior margin. Epibranchial 3 with dorsally curved uncinate process on posterior margin and 0-1 ventral gill raker just lateral to uncinate process. Ceratobranchial 4 with 5-6 gill rakers along anterior and posterior margins. Epibranchial 4 with 0-1 gill raker along anteroventral margin. Upper dentigerous plate with 16-17 conical teeth arranged in up to two rows along anterior half of bone and one row posteriorly. Teeth along single posterior row largest. Ceratobranchial 5 with 4-5 gill rakers along anterior margin and 15-18 conical teeth, along medial margin of anterior portion, arranged in up to two irregular rows. Largest teeth posteromedially placed.

Supraorbital sensory canal interrupted at nasal region with four pores (52*), and not connected to its counterpart through medial commissure. Nasal section of supraorbital canal continuous with frontal section in both sides in 8 specimens and in only one side in 11 specimens. Sensory pore s1 medially adjacent to anterior nostril; s2 and s3 medial to posterior nostril; s6 (epiphyseal) paired, immediately adjacent to main canal. Infraorbital sensory canal interrupted in two sections; anteriormost section with sensory pores i1 and i3, laterally adjacent to anterior and posterior nostrils, respectively; posteriormost section connected to supraorbital and otic canals, with a single terminal sensory pore (56*) at end of very short branch, extending from postorbital process. Four specimens with two sensory pores in posteriormost section of infraorbital canal in both sides, and in only one side in 11 specimens. Preopercular canal short with single terminal pore antero-dorsal to opercular patch of odontodes. Pterotic branch of postotic canal present with associated pore above opercular patch of odontodes. Tunk canal short with two pores above pectoral-fin base. Sensory pore ll1 ventral to trunk line canal and ll2 at terminus of trunk canal.

Precaudal free vertebrae 8-9 and caudal vertebrae 28-29, totaling 37 vertebrae. Ribs 12-14. First hemal spine on vertebra 16. Anus at vertical through posterior third of dorsal-fin base, approximately at level of base of fifth branched ray.

Pectoral fin with i, 7-8 rays (a single specimen of 41.2 mm SL from IAvH-P 15813 with six branched rays on left side). First ray longest, projected beyond margin of fin as a long filament (*ca*. 40% longer than second pectoral-fin ray). Remaining rays gradually shorter medially. Pectoral complex radial cartilaginous. Coracoid bridge (scapulocoracoid process) pointed. Posterior lamina of cleithrum lacking foramina.

Pelvic fin with i, 4 (68) rays or i, 2-3 (one specimen of 41.2 mm SL from IAvH-P 15813), and short lateral splint, its length around one sixth of first ray length. Pelvic-fin insertion slightly anterior to dorsal-fin origin, at level of free vertebra 17 or 18. Second and third rays longest. Inner margins of pelvic-fin bases in contact. Posterior tip of fin reaching urogenital papilla. Basipterygium with two anterior long processes of around same length. Larger CS specimen (IAvH-P 15813) with shorter anteromedial process.

Dorsal fin with 3-4 procurrent rays and ii, 6 (2), 7* (48), 8 (18) principal rays. Shape of fin rectangular in lateral view, posterior margin rounded. First and second branched rays longest. Origin of fin posterior to pelvic-fin insertion. Basal and anterior portions of fin covered by thick integument. Supporting elements of dorsal fin represented by eight basal radials, inserted between neural spines of vertebrae 16-21, and six distal radials, associated with second to penultimate basal radials.

Anal fin with 3 procurrent rays and ii, 2 (1), 4 (3), 5* (56), 6 (7) principal rays. Anal fin similar in shape to dorsal fin, but smaller. First and second branched rays longest. Origin of fin entirely

behind dorsal-fin base. Base and anterior portion of fin similarly covered by thick integument as in dorsal fin. Basal radials six (IAvH-P 15809 CS specimen with a seventh basal radial, less than half length of preceding basal radial, independently associated with last anal-fin ray), inserted between hemal spines of vertebrae 20-24. Distal radials four, associated with second to penultimate basal radials.

Caudal-fin margin rounded, with dorsal rays longer. Caudal fin with i, 5+6, i* (65) or i, 10, i (1) or i, 9, i (1) principal rays. Dorsal procurrent rays 20-21, inserted posterior to neural spine of vertebra PU9. Ventral procurrent rays 13-17, inserted posterior to hemal spine of vertebrae PU8 or PU9. Posteriormost ventral procurrent ray entirely segmented and articulating with caudal skeleton. Caudal skeleton with three plates (PH+1+2, 3, 4+5). Ventral plate (PH+1+2) larger than upper plates (3 and 4+5). Nodular epural present but partially fused to urostyle in IAvH-P 15809 CS specimen. Neural spine of compound caudal vertebra complete and fused posteriorly to urostyle (IAvH-P 15813 CS specimen with incomplete neural spine).

Color in alcohol. Body lacking dark integumentary pigment, uniformly light yellow to cream, distal region of fins hyaline (Figure 1).

Color in life. Dorsal and lateral portion of body and lateral portion of head (cheek) pinkish, showing a greenish iridescent aspect on dorsal surface of head, fins, and caudal peduncle. Distal margin of fins hyaline (Figure 7).

Etymology. The specific name is used as a noun in apposition in reference to the Rosablanca karstic formation where the type locality is found.

Distribution and habitat. *Trichomycterus rosablanca* is known exclusively from a stream tributary of the Horta River, draining the caves Las Sardinas and Caracol, in the upper Carare River drainage, corresponding to the middle Magdalena River basin (Figure 8). The caves Las Sardinas and Caracol are found between 2228 m and 2378 m of elevation. The subterranean stream draining the caves have clear waters, becoming turbid during the rains by heavy loads of clayey sediments. Physicochemical parameters measured during the collecting dates were the following: temperature 14.6°C, pH 7.9 in Las Sardinas Cave and 8.1 in Caracol Cave, total dissolved solids 132 ppm in both caves, and conductivity 231 µ/cm in Las Sardinas Cave and 242 µ/cm in Caracol Cave. *Trichomycterus rosablanca* was collected in a 20 m section of the stream that drains into a sink hole inside the wide opening gallery of Caracol Cave (Figure 9). Las Sardinas Cave has two openings (Figure 10, Figure 11) that are interconnected by a superficial stream flowing for around 200 m from the northern opening and inflowing the second southern opening (Figure 10). The specimens were collected at 230 m (dark section) inside the northern opening and in the epigean section of the interconnecting stream (Figure 8, Figure 9). Collecting efforts both in the epigean and hypogean systems failed to capture any other fish species in the region. This system of caves is part of the Rosablanca formation (Mendoza-Parada *et al*., 2009).

Figure 7. Live specimens of *Trichomycterus rosablanca* (left picture corresponds to one specimen coming from IAvH-P 15811 lot of paratypes). Photographs by Felipe Villegas.

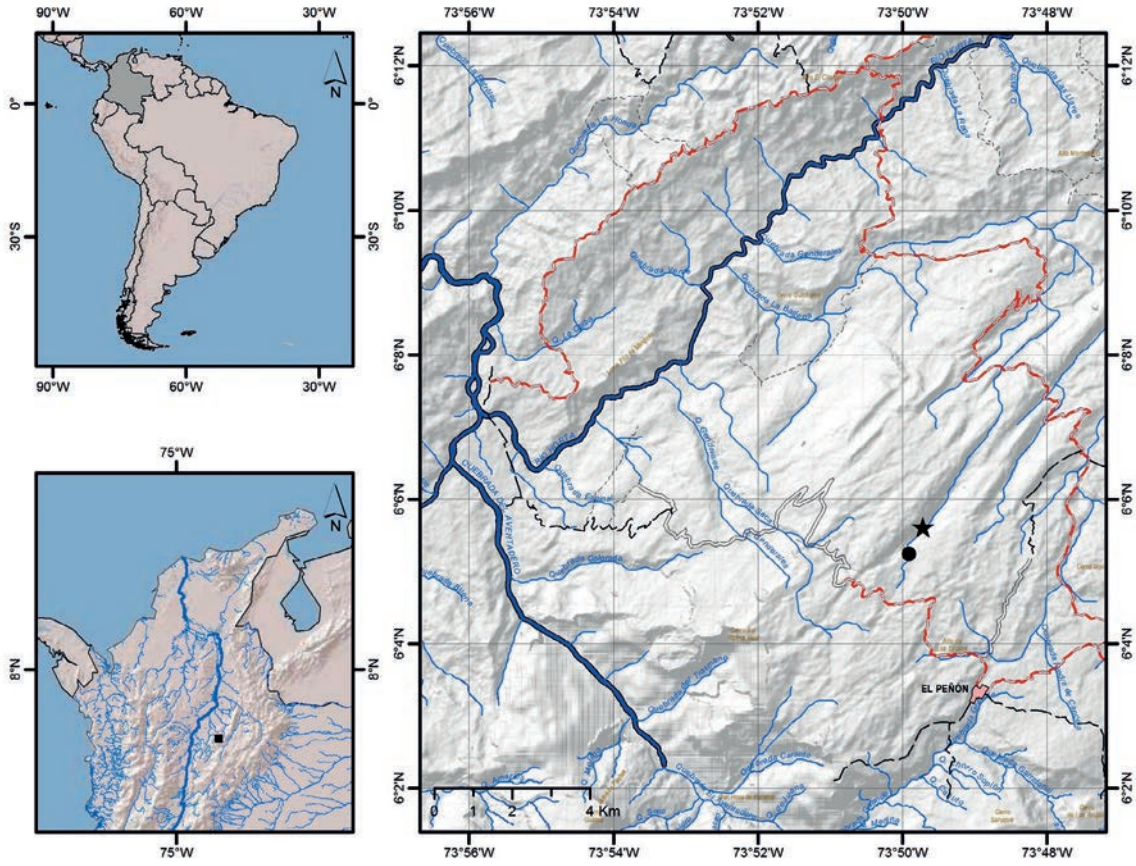

Figure 8. Maps of middle basin of the Magdalena River (left lower inset) and Horta River drainage (right), showing collecting localities of *Trichomycterus rosablanca* (type locality star).

Figure 9. Caracol Cave. A. Opening. B. Underground waterfall.

Figure 10. Satellite image showing location of Las Sardinas (Cs1, Cs2) and Caracol (Cc3) caves. Source: Google Earth (accessed 22 May 2017). Edited by Jesús Fernández Auderset.

Figure 11. Las Sardinas Cave. A. Output channel. B. Las Sardinas Creek. C. Subterranean creek. Photograph B by Rodrigo Barbella.

Genetic identification. The resulting alignment of the COI gene sequences consisted of 618 bp, with no insertions, deletions or stop codons. Nucleotide frequencies were 25.3% adenine, 27.7% cytosine, 17.9% guanine, and 29.2% thymine. Considering all base positions, 406 sites were invariant, 216 were polymorphic, and 157 were parsimony informative. The mean K2P distance between species was 0.138, while the mean divergence between *Trichomycterus* species was lower (0.117±0.009). The maximum distance was found between *T. rosablanca* and *T. sandovali* with 24.7% (Table 3). The two sequences of *T. rosablanca* did not show intraspecific variation. Graphical structure of the distance data is shown in the NJ tree (Figure 12), indicating that *T. rosablanca* is closer to *Eremophilus mutisii* and represents a distinct lineage from the other trans-Andean species analyzed (including the most similar in general appearance *T. sandovali*). The tree topology of the GMYC analysis is identical to that shown in the Figure 12 and indicates the presence of 17 operational taxonomic units, with a threshold time of 0.0003512371, which indicates the time before which all nodes represent diversification events and after which all nodes in the tree reflect coalescent events. The likelihood of the null model was 65.8095 and the maximum likelihood of the GMYC model was 67.05544. Genetic divergence and delimitation species analyses indicate that all species examined possess COI sequences that allow their mutual recognition.

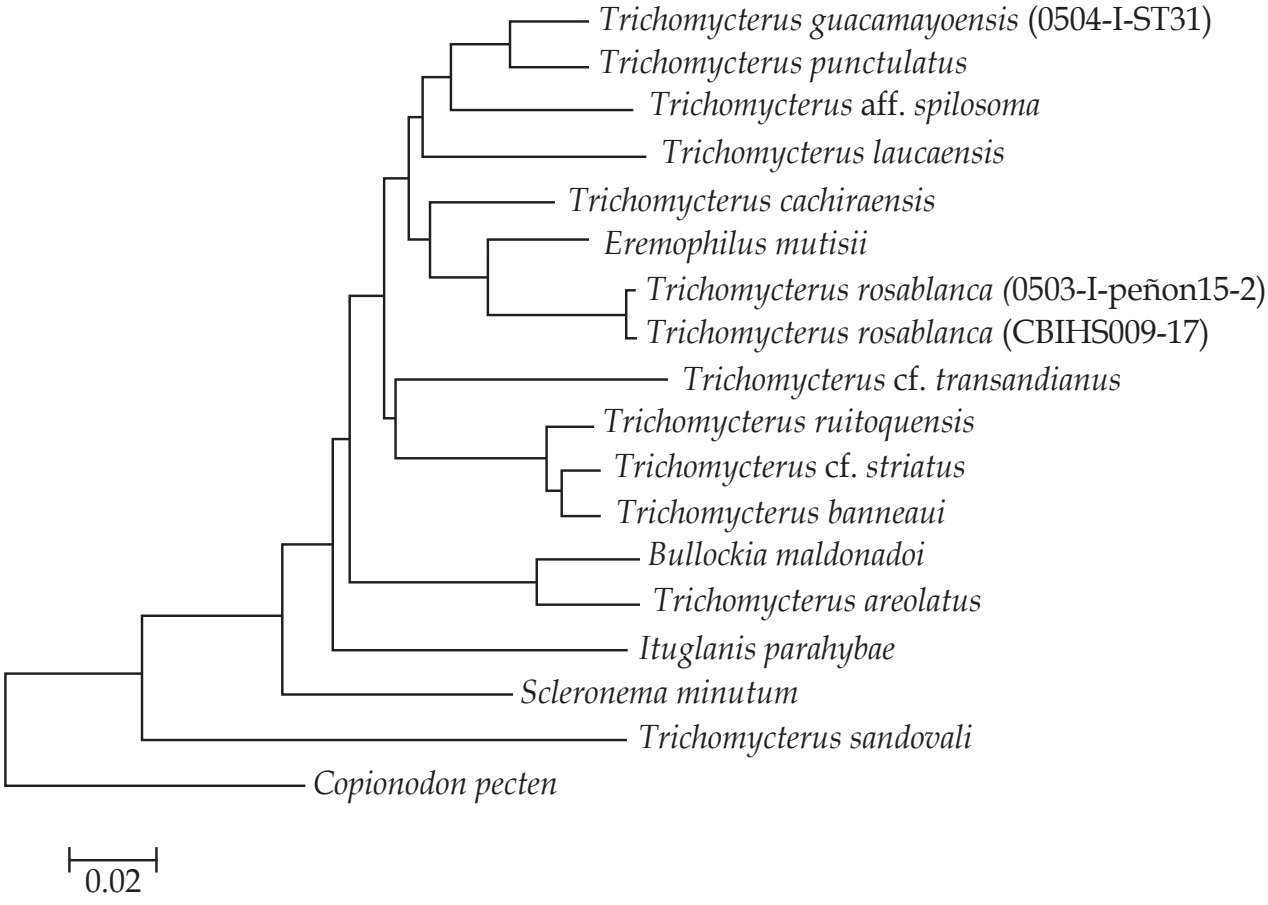

Figure 12. Neighbour-joining tree of COI sequence divergence (K2P) in 17 trichomycterid species, including *Trichomycterus rosablanca* and *T. sandovali*.

Table 3. Pairwise comparison of nucleotide divergence (K2P distances) at COI from 17 representative species of Trichomycteridae, including *Trichomycterus rosablanca* and *T. sandovali*.

	Species	1	2	3	4	5	6	7	8	9	10	11	12	13	14	15	16	17
1	*Copionodon pecten*																	
2	*Bullockia maldonadoi*	0.239																
3	*Scleronema minutum*	0.207	0.151															
4	*Ituglanis parahybae*	0.228	0.144	0.142														
5	*Eremophilus mutisii*	0.241	0.130	0.136	0.141													
6	*Trichomycterus rosablanca* 0503-I-peñon15-2 (IAvH-P 15811)	0.240	0.142	0.153	0.152	0.058												
7	*Trichomycterus rosablanca* CBIHS009-17 (IAvH-P 15811)	0.240	0.139	0.152	0.152	0.057	0.000											
8	*Trichomycterus areolatus*	0.226	0.048	0.149	0.145	0.127	0.144	0.141										
9	*Trichomycterus laucaensis*	0.220	0.137	0.124	0.148	0.107	0.135	0.116	0.125									
10	*Trichomycterus punctulatus*	0.209	0.138	0.131	0.134	0.085	0.081	0.079	0.133	0.096								
11	*Trichomycterus guacamayoensis* CBIHS010-17 (IAvH-P 13984)	0.209	0.142	0.135	0.132	0.079	0.081	0.079	0.137	0.098	0.035							
12	*Trichomycterus banneaui*	0.200	0.131	0.140	0.126	0.098	0.113	0.111	0.140	0.125	0.100	0.092						
13	*Trichomycterus cachiraensis*	0.212	0.118	0.133	0.127	0.068	0.081	0.079	0.107	0.091	0.081	0.087	0.101					
14	*Trichomycterus* aff. *spilosoma*	0.229	0.151	0.133	0.149	0.092	0.102	0.100	0.141	0.101	0.072	0.080	0.127	0.087				
15	*Trichomycterus* cf. *striatus*	0.195	0.138	0.138	0.130	0.096	0.107	0.105	0.144	0.127	0.094	0.092	0.018	0.094	0.119			
16	*Trichomycterus* cf. *transandianus*	0.234	0.144	0.140	0.154	0.135	0.135	0.132	0.155	0.138	0.125	0.117	0.111	0.105	0.131	0.119		
17	*Trichomycterus ruitoquensis*	0.204	0.129	0.136	0.128	0.113	0.113	0.111	0.138	0.109	0.100	0.096	0.020	0.087	0.117	0.025	0.117	
18	*Trichomycterus sandovali*	0.225	0.220	0.198	0.233	0.236	0.247	0.246	0.227	0.241	0.226	0.243	0.223	0.223	0.246	0.233	0.251	0.224

Discussion

The genus *Trichomycterus* is one of the most challenging Neotropical fish groups in terms of uncovering its actual taxonomic diversity and the phylogenetic relationships of its constituent species, given two main limiting factors: 1) complex taxonomic history coupled with incomplete taxonomic inventory, and 2) polyphyletic nature, a contentious issue that is broadly agreed upon and reiteratively corroborated (de Pinna, 1998). Recently, Ochoa *et al.* (2017) published a multilocus analysis of Trichomycteridae, with a comprehensive taxonomic sampling of trichomycterine representatives, confirming the polyphyletic status of *Trichomycterus*. However, it also revealed a series of subclades with some clear geographic circumscriptions. This molecular analysis corroborated an important input to the systematics of trichomycterids by recovering a monophyletic Trichomycterinae, as previously defined on morphological grounds by Datovo and Bockmann (2010), i.e. containing *Ituglanis* Costa & Bockmann, 1993 and *Scleronema* Eigenmann, 1918. *Trichomycterus rosablanca* shares the apomorphic condition of the origin of the *levator internus 4* attached to the dorsal face of the posttemporo-supracleithrum, the single morphological synapomorphy of Trichomycterinae proposed so far (Datovo & Bockmann, 2010), although it must be noted that some *Trichomycterus* species present the plesiomorphic character state (García-Melo *et al.*, 2016).

A high proportion (73%) of the analyzed specimens (71) of *Trichomycterus rosablanca* shows an interrupted supraorbital canal at the nasal section, giving origin to four sensory pores (s1, s2, s3, and s6), which represents an apomorphic condition of the cephalic laterosensory system for trichomycterids. Remaining specimens (19) exhibit the plesiomorphic condition, represented by an uninterrupted supraorbital canal, with most specimens (11) having an asymmetric pattern (i.e. on only one side). This pattern of the cephalic laterosensory system is not found in congeners from northern South America (Colombia and Venezuela), but is shared by the Andean species *T. aguarague* Fernández & Osinaga, 2006; *T. alterus* (Marini, Nichols & La Monte, 1933); *T. areolatus* Valenciennes, 1846; *T. belensis* Fernández & Vari, 2002; *T. chiltoni* (Eigenmann, 1920); *T. chungaraensis* Arratia, 1983; *T. dispar* (Tschudi, 1846); *T. heterodontus* (Eigenmann, 1918); *T. laucaensis*; *T. megantoni* Fernández & Quispe Chuquihuamaní, 2007; *T. minus* Fernández & Vari, 2012; *T. punctulatus*; *T. ramosus* Fernández, 2000; *T. rivulatus* Valenciennes, 1846; and *T. vittatus* Regan, 1903 (Arratia, 1998; Fernández, 2006; DoNascimiento *et al.*, 2014a). Such condition has a homoplastic distribution within Trichomycteridae, being also found in *Trichogenes* Britski & Ortega, 1983; *Eremophilus* Humboldt, 1805; *Hatcheria* Eigenmann, 1909 [although Arratia and Huaquin (1995) recorded a continuous supraorbital canal reaching the sensory pore s1 in *Hatcheria macraei* (Girard, 1855), Figure 8F, p. 20]; *Ituglanis boitata* Ferrer, Donin & Malabarba, 2015 (Ferrer *et al.*, 2015: Figure 2, p. 380); *I. eichorniarum* (Miranda Ribeiro, 1912); *I. ina* Wosiacki, Dutra & Mendonça, 2012 (Rizzato & Bichuette, 2016); *I. paraguassuensis* (Campos-Paiva & Costa, 2007: Figure 2, p. 55); *I. proops* (Miranda Ribeiro, 1908) (Sarmento-Soares *et al.*, 2006: p. 317); *Scleronema*, *Tridensimilis* Schultz, 1944; Stegophilinae; and Vandelliinae. However, this character could still be informative for less inclusive clades within Trichomycterinae, as suggested by the results depicted in the NJ tree obtained for the analyzed COI sequences (Figure 12), where *T. rosablanca* is placed as sister to *E. mutisii*. Both species share the apomorphic interrupted nasal section of the supraorbital canal, in spite of the intraspecifically variable condition in *T. rosablanca*. This placement of *T. rosablanca* adds to the growing evidence of the non-monophyletic status of *Trichomycterus* as currently defined, requiring further extensive studies with a greater taxonomic sampling, in order to identify and diagnose subsets of *Trichomycterus* more closely related with other trichomycterine genera (e.g. *Eremophilus*) than to remaining species of *Trichomycterus*.

Another derived character shown by *Trichomycterus rosablanca* consists of the lachrimal/antorbital bone not enclosing the infraorbital canal (Figure 3). Plesiomorphically the anteriormost section of the infraorbital canal (bearing the sensory pores i1 and i3) is enclosed by a hollow posterior section of the lachrimal/antorbital. This bone in *T. rosablanca* apparently lost its tubular posterior section, remaining as a compact bone still attached through a posterior pointed process to the anteroventral margin of the infraorbital canal. A slightly different condition is verified in *T. arleoi* (Fernández-Yépez, 1972) and *T. mondolfi* (Schultz, 1945), where the anteriormost section of the infraorbital canal is also free from the lachrimal/antorbital, but the bone is completely detached from the infraorbital canal, having lost its posterior tubular portion and keeping only the anteriormost compact portion that is associated with the anterolateral corner of the anterior cartilage of the autopalatine. The phylogenetic relationships of *T. arleoi* and *T. mondolfi* plus two closely related undescribed species are being addressed in an ongoing study by C. DoNascimiento (in prep.).

Aside from the obvious troglomorphisms present in *Trichomycterus rosablanca*, this species is furthermore diagnosed from remaining trichomycterines by two putative autapomorphies. The first diagnostic character is the presence of a conspicuous foramen in the main body of the interopercle that communicates the anterior and posterior surfaces of the bone (Figure 2A), being the plesiomorphic character state a compact interopercle, lacking of any foramina (Figure 2B). The interopercular foramen was consistently found in all three CS specimens of *Trichomycterus rosablanca*. Asymmetric presence of the foramen was observed in one of the three examined specimens, but even this specimen has a well-developed foramen on one side, such as that found on both sides of the two remaining specimens. On the other hand, this foramen has not been observed in more than 100 directly examined specimens, representing almost 60 species of *Trichomycterus* (listed in DoNascimiento *et al*., 2014a, b; DoNascimiento 2015; García-Melo *et al*., 2016) that come from different major river basins across the distributional range of the genus (both cis and trans-Andean species, from Panama to Argentina). Likewise, this character has not been previously recorded in those species where osteological information and illustrations of the interopercle have been provided. A similar foramen is found in *Potamoglanis* Henschel, Mattos, Katz & Costa, 2017; the tridentines *Tridensimilis* and *Tridentopsis* Myers, 1925; and the stegophilines *Acanthopoma* Lütken, 1892; *Henonemus* Eigenmann & Ward, 1907; *Homodiaetus* Eigenmann & Ward, 1907; *Ochmacanthus* Eigenmann, 1912; *Pareiodon* Kner, 1855; *Pseudostegophilus* Eigenmann & Eigenmann, 1889; and *Schultzichthys* Dahl, 1960. Given the distant phylogenetic position of the implied taxa (*Potamoglanis*, Tridentinae, and Stegophilinae) from the inferred placement of *T. rosablanca* within Trichomycterinae, these occurrences are best interpreted as independent acquisitions.

The second autapomorphy (although intraspecifically variable in a relatively small proportion, 5.6% of 71 studied specimens) is the presence of a single sensory pore at the posteriormost section of the infraorbital canal. Most trichomycterids (non-trichogenines, non-copionodontines) with an interrupted infraorbital canal have two sensory pores, i10 and i11. *Potamoglanis*, an undescribed species of *Tridens* from the Colombian Amazon, *Tridensimilis*, Stegophilinae, Vandelliinae, *Sarcoglanis*, and *Glanapteryx* also have a single sensory pore in this section of the infraorbital canal. Once again, this homoplastic pattern is more parsimoniously interpreted as two independent losses, one in the TSVSG clade, which includes the subfamilies Tridentinae, Stegophilinae, Vandelliinae, Sarcoglanidinae, and Glanapteryginae (Costa and Bockmann, 1993; Ochoa *et al*., 2017), and another in *T. rosablanca* within trichomycterines.

The restricted distribution of *Trichomycterus rosablanca* to hypogean systems framed by an environmental mosaic, where the agricultural

frontier has advanced notably, has resulted in a fragmented landscape, with surrounding forests pushed to the higher and inaccessible mountain tops. Deforestation and consequent increase of sedimentation, coupled with indiscriminate fumigation of crops and cattle pastures that drain contaminants into the hydric system of the caves, place the conservation status of *T. rosablanca* at risk. Therefore, additional studies to determine the vulnerability of this species are promptly required.

Acknowledgements

We are grateful to Jesús Fernández Auderset (Espeleo Colombia), Camilo Chica, Camilo Martínez-Martínez (Cromatophoro), Gabriel Vargas, Michael Galeano, and Rodrigo Barbella for their invaluable help in the field; Felipe Villegas for the photographs of the holotype and live specimens; Diego Córdoba for the map; Eduardo Tovar Luque for sequencing the tissue samples of *Trichomycterus rosablanca*; Paola Pulido-Santacruz for publishing the COI sequence of *T. rosablanca* in BOLD and GenBank and Mailyn Adriana González for her support at the Biodiversity Science Program of the Humboldt Institute. Funding was granted by the *Convenio Especial de Colaboración Colciencias - Instituto de Investigación de Recursos Biol*ógicos Alexander von Humboldt # *FP44842-109-2016* (IAvH 16-062).

Literature cited

Arratia, G. (1983). *Trichomycterus chungaraensis* n. sp. and *Trichomycterus laucaensis* n. sp. (Pisces, Siluriformes, Trichomycteridae) from the high Andean range. *Studies on Neotropical Fauna and Environment*, 18 (2): 65-87.

Arratia, G. (1998). *Silvinichthys*, a new genus of trichomycterid catfishes from the Argentinian Andes, with redescription of Trichomycterus nigricans. *Ichthyological Exploration of Freshwaters*, 9 (4): 347-370.

Arratia, G & Huaquin, L. (1995). Morphology of the lateral line system and of the skin of diplomystid and certain primitive loricarioid catfishes and systematic and ecological considerations. *Bonner Zoologische Monographien,* 36: 1-110.

Campos-Paiva, R. M. & Costa, W. J. E. M. (2007). *Ituglanis paraguassuensis* sp. n. (Teleostei: Siluriformes: Trichomycteridae): a new catfish from the rio Paraguaçu, northeastern Brazil. *Zootaxa*, 1471: 53-59.

Chakrabarty, P., Warren, M., Page, L. M. & Baldwin, C. C. (2013). GenSeq: An updated nomenclature and ranking for genetic sequences from type and non-type sources. *ZooKeys*, 346: 29-14.

Costa, W. J. E. M. & Bockmann, F. A. (1993). Un nouveau genre néotropical de la famille des Trichomycteridae (Siluriformes: Loricarioidei). *Revue Française d'Aquariologie -Herpétologie*, 20 (2): 43-46.

Datovo, A. & Bockmann, F. A. (2010). Dorsolateral head muscles of the catfish families Nematogenyidae and Trichomycteridae (Siluriformes: Loricarioidei): comparative anatomy and phylogenetic analysis. *Neotropical Ichthyology*, 8 (2):193-246.

DoNascimiento, C. (2015). Morphological evidence for the monophyly of the subfamily of parasitic catfishes Stegophilinae (Siluriformes, Trichomycteridae) and phylogenetic diagnoses of its genera. *Copeia*, 103 (4): 933-960.

DoNascimiento, C., Prada-Pedreros, S. & Guerrero-Kommritz, J. (2014a). *Trichomycterus venulosus* (Steindachner, 1915), a junior synonym of *Eremophilus mutisii* Humboldt, 1805 (Siluriformes: Trichomycteridae) and not an extant species. *Neotropical Ichthyology,* 12 (4): 707-715.

DoNascimiento, C., Prada-Pedreros, S. & Guerrero-Kommritz, J. (2014b). A new catfish species of the genus *Trichomycterus* (Siluriformes: Trichomycteridae) from the río Orinoco versant of Páramo de Cruz Verde, Eastern Cordillera of Colombia. *Neotropical Ichthyology*, 12 (4): 717-728.

Drummond, A. J., Ho, S. Y. W., Phillips, M. J. & Rambaut, A. (2006). Relaxed phylogenetics and

dating with confidence. *PLoS Biology*, 4 (5): e88. https://doi.org/10.1371/journal.pbio.0040088.

Drummond, A. J., Suchard, M. A., Xie, D. & Rambaut, A. (2012). Bayesian phylogenetics with BEAUti and the BEAST 1.7. *Molecular Biology and Evolution*, 29 (8): 1969-1973.

Eschmeyer, W. N. & Fong, J. D. (2017). Species by family/subfamily. Retrieved on August 22, 2017 from http://researcharchive.calacademy.org/research/ichthyology/catalog/SpeciesByFamily.asp.

Fernández, L. A. (2006). Two new patterns of the supraorbital canal in trichomycterids (Siluriformes: Trichomycteridae). *Acta Zoológica Lilloana*, 50: 115-117.

García-Melo, L. J., Villa-Navarro, F. A. & DoNascimiento, C. (2016). A new species of *Trichomycterus* (Siluriformes: Trichomycteridae) from the upper río Magdalena basin, Colombia. *Zootaxa*, 4117 (2): 226-240.

Kimura, M. (1980). A simple method for estimating evolutionary rates of base substitutions through comparative studies of nucleotide sequences. *Journal of Molecular Evolution*, 16 (2): 111-120.

Kumar, S., Stecher, G. & Tamura, K. (2016). MEGA7: Molecular Evolutionary Genetics Analysis version 7.0 for bigger datasets. *Molecular Biology and Evolution*, 33 (7): 1870-1874.

Lundberg, J. G. & Baskin, J. N. (1969). The caudal skeleton of the catfishes, Order Siluriformes. *American Museum Novitates,* 2398: 1-49.

Mendoza-Parada, J. E., Moreno-Murillo, J. M. & Rodríguez-Orjuela, G. (2009). Sistema cárstico de la Formación Rosablanca Cretácico inferior, en la provincia de Vélez, Colombia. *Geología Colombiana*, 34: 35-44.

Morris, P. J., Yager, H. M. & Sabaj Pérez, M. H. (2006). ACSImagebase: a digital archive of catfish images compiled by participants in the All Catfish Species Inventory. [WWW image Database] URL http://acsi.acnatsci.org/base.

Ochoa, L., Roxo, F., DoNascimiento, C., Sabaj, M., Datovo, A., Alfaro, M. & Oliveira, C. (2017). Multilocus analysis of the catfish family Trichomycteridae (Teleostei: Ostariophysi: Siluriformes) supporting a monophyletic Trichomycterinae. *Molecular Phylogenetics and Evolution*, 115: 71-81.

de Pinna, M. C. C. (1992). *Trichomycterus castroi*, a new species of trichomycterid catfish from the Rio Iguaçu of Southeastern Brazil (Teleostei: Siluriformes). *Ichthyological Exploration of Freshwaters*, 3 (1): 89-95.

de Pinna, M. C. C. (1998). Phylogenetic relationships of neotropical Siluriformes: historical overview and synthesis of hypotheses. In Malabarba, L. R., Reis, R. E., Vari, R. P., Lucena, Z. M. S. & Lucena, C. A. S. (Eds.). *Phylogeny and classification of Neotropical fishes*. Pp. 279-330. Porto Alegre: EDIPUCRS. 603 p.

de Pinna, M. C. C. & Wosiacki, W. (2003). Trichomycteridae. In Reis, R. E., Kullander, S. O. & Ferraris Jr., C. J. (Eds.). *Check list of the Freshwater Fishes of South and Central America*. Pp. 270-290. Porto Alegre: EDIPUCRS. 742 p.

Rizzato, P. P. & Bichuette, M. E. (2016). The laterosensory canal system in epigean and subterranean *Ituglanis* (Siluriformes: Trichomycteridae), with comments about troglomorphism and the phylogeny of the genus. *Journal of Morphology*, 278 (1): 4-28.

Sarmento-Soares, L. M., Martins-Pinheiro, R. F., Aranda, A. T. & Chamon, C.C. (2006). *Ituglanis cahyensis*, a new catfish from Bahia, Brazil (Siluriformes: Trichomycteridae). *Neotropical Ichthyology,* 4 (3): 309-318.

Schaefer, S. A. & Aquino, A. E. (2000). Postotic laterosensory canal and pterotic branch homology in catfishes. *Journal of Morphology*, 246: 212-227.

Taylor, W. R. & Van Dyke, G. C. (1985). Revised procedures for staining and clearing small fishes and other vertebrates for bone and cartilage study. *Cybium*, 9: 107-119.

Lina M. Mesa S.
Programa Ciencias Básicas de la Biodiversidad,
Instituto de Investigación de Recursos Biológicos
Alexander von Humboldt
Bogotá, Colombia
lmesa@humboldt.org.co

Carlos A. Lasso
Programa Ciencias Básicas de la Biodiversidad,
Instituto de Investigación de Recursos Biológicos
Alexander von Humboldt
Bogotá, Colombia
classo@humboldt.org.co

Luz. E. Ochoa
Departamento de Morfologia, Instituto de Biociências,
UNESP - Universidade Estadual Paulista "Julio de
Mesquita Filho"
São Paulo, Brasil
luzeocho@gmail.com

Carlos DoNascimiento
(Autor de correspondencia)
Colecciones Biológicas,
Instituto de Investigación de Recursos Biológicos
Alexander von Humboldt
Villa de Leyva, Boyacá, Colombia
cdonascimiento@humboldt.org.co

Trichomycterus rosablanca (Siluriformes, Trichomycteridae) a new species of hipogean catfish from the Colombian Andes

Citación del artículo: Mesa S., L. M., Lasso, C. A., Ochoa, L. E. y DoNascimiento, C. (2018). *Trichomycterus rosablanca* (Siluriformes, Trichomycteridae) a new species of hipogean catfish from the Colombian Andes. *Biota Colombiana*, 19 (Sup. 1): 95-116. DOI: 10.21068/c2018.v19s1a09. http://zoobank.org/urn:lsid:zoobank.org:pub:4ACC4A1E-39DF-4D40-A51A-0E023E02D37F

Recibido: 31 de agosto de 2017
Aprobado: 30 de enero de 2018